INFUB - 11th European Conference on Industrial Furnaces and Boilers, INFUB-11

Study on the influence of ethanol and butanol addition on soot formation in iso-octane flames

I. Frenzel[a],*, H. Krause[a], D. Trimis[b,a]

[a]TU Bergakademie Freiberg, Institute of Thermal Engineering, Gustav-Zeuner-Strasse 7, 09599 Freiberg, Germany
[b]Karlsruhe Institute of Technology, Engler-Bunte-Institute, Division of Combustion Technology, Engler-Bunte-Ring 1, 76131 Karlsruhe, Germany

Abstract

The emphasis of the work was to study the influence of ethanol and n-butanol addition on soot formation in the combustion process of iso-octane. Soot particle size distribution functions were measured at different heights above the burner in selected fuel-rich atmospheric pressure laminar premixed iso-octane/ethanol and iso-octane/n-butanol flames. The results showed that the addition of both alkanols to the reference fuel iso-octane reduces the soot formation potential in the flames. The comparison of the particle size distribution functions indicated that both the process of soot particle nucleation in the lower heights of the flame and coagulation in the larger heights of the flame are influenced by the positive effect of the addition of the oxygenated fuels. When comparing the influence of ethanol and n-butanol, it is obvious that n-butanol addition leads to a higher reduction of soot formation in iso-octane flames.

Keywords: Soot formation; laminar premixed flames; soot particle size distribution functions; iso-octane; influence of ethanol and n-butanol

1. Introduction

The legislation for soot particle emissions has become stricter by limiting not only the mass but also the total number of particles. At the same time the use of biofuels in gasoline engines is of increasing importance to reduce the global CO_2 emissions from vehicles [1]. Since the combustion of biofuels leads to different soot emissions

---

* Corresponding author. Tel.: +49-3731-39-3013; fax: +49-3731-39-3942.
E-mail address: Isabel.Frenzel@iwtt.tu-freiberg.de

compared to classical gasoline, the scope of this study is the investigation of the underlying physical and chemical phenomena leading to these differences. The best-known representatives of these biofuels are methanol, ethanol and butanol that are produced via fermentation of sugar cane and crops and belong to the group of alkanols. For spark-ignition engines renewable bio-ethanol is mainly used as surrogate in several countries (e. g. Brazil, USA and European Union). Additionally, butanol is considered, because of its higher energy content. Butanol has four isomers, however, actually the use of n-butanol is promoted due to the fact, that it can be easily produced with a retrofitting of existing ethanol production facilities.

The different physical and chemical properties of the bio-components in the fuel have a high impact on the combustion process in engines and affect the soot formation and therefore the soot particle emissions from vehicles as well. In general, the addition of oxygenated fuels reduces the particle emissions [2,3,4,5], but in other studies contradictory trends were observed [6,7]. Karavalkis et al. [8] and Lee et al. [9] found out that low alkanol contents in the fuel did not necessarily show particulate matter mass reduction. Additionally, it was shown in [8] that the fuel with the highest oxygen levels leads to the highest decrease of particle emissions of vehicles. However, these global analyses with special engine geometries and operating points do not allow general statements regarding the soot particle emissions. Due to the complex behavior of the fuel mixtures there is a leak of knowledge in the engine combustion process chain and therefore a forecast of soot formation for single fuels and different operating conditions is still not possible.

In this work pure iso-octane, known as primary reference fuel in engine combustion research, was used as reference fuel and the influence of ethanol and n-butanol addition was studied in detail to investigate the underlying physical and chemical phenomena leading to the differences in soot formation when an alkanol is added. The investigations were carried out under simplified conditions in lab-scale flames to obtain experimental data without the influence of the complex interactions in an engine and therefore to provide data for modeling purposes.

The influence of ethanol addition on flame structure, gas composition and soot formation in the premixed lab-scale combustion of several short-chain hydrocarbon fuels has been already studied by different groups. Wu et al. [10] and Salamanca et al. [11] investigated premixed laminar ethylene flames in a flat-flame burner and observed that the addition of ethanol reduces the soot particle formation. Camacho et al. [12] studied the differences in the soot formation in laminar premixed pure iso-butanol and n-butanol flames. However, no experimental data is available for the influence of ethanol and n-butanol addition on soot formation in flat flames of higher hydrocarbons such as iso-octane. Therefore the emphasis of this work was to investigate various blends and to analyze the influence of biofuel addition on soot particle formation in detail. The utilized experimental setup consisted of a McKenna burner [13] and a suitable system for supplying and conditioning of fuel and oxidizer. Soot particle size distribution functions (PSDF) were measured at different heights above the burner (HAB) in selected fuel-rich atmospheric pressure laminar premixed flames using an in situ probe sampling and a suitable gas conditioning system (similar to [14]) for online analysis with a scanning mobility particle sizer (SMPS).

2. Experimental setup and method

The experimental setup used in this study is described in the following and is schematically shown in Figure 1. The investigated flames were stabilized on a commercial oil-cooled McKenna burner (provided by Holthuis & Associates [13]) that consists of an inner sintered porous bronze plug (inner diameter 60 mm) and an outer concentric annulus for shroud gas shielding the flame from the atmosphere. A stabilization plate made of stainless steel was placed 50 mm above the burner plate to further stabilize the flames.

The conditions of all studied flames are summarized in Table 1. In addition to four iso-octane/ethanol and two iso-octane/n-butanol blends (e.g. B20 means 20 vol.-% of liquid n-butanol in iso-octane), pure iso-octane, ethanol and n-butanol were used as fuels as well. The equivalence ratio was fixed at $\phi = 2.3$ for all investigated flames and the superficial cold gas velocity of the unburnt gas mixture of all flames was 5 cm/s at 273 K and 1 atm (in an empty cylinder of the same diameter).
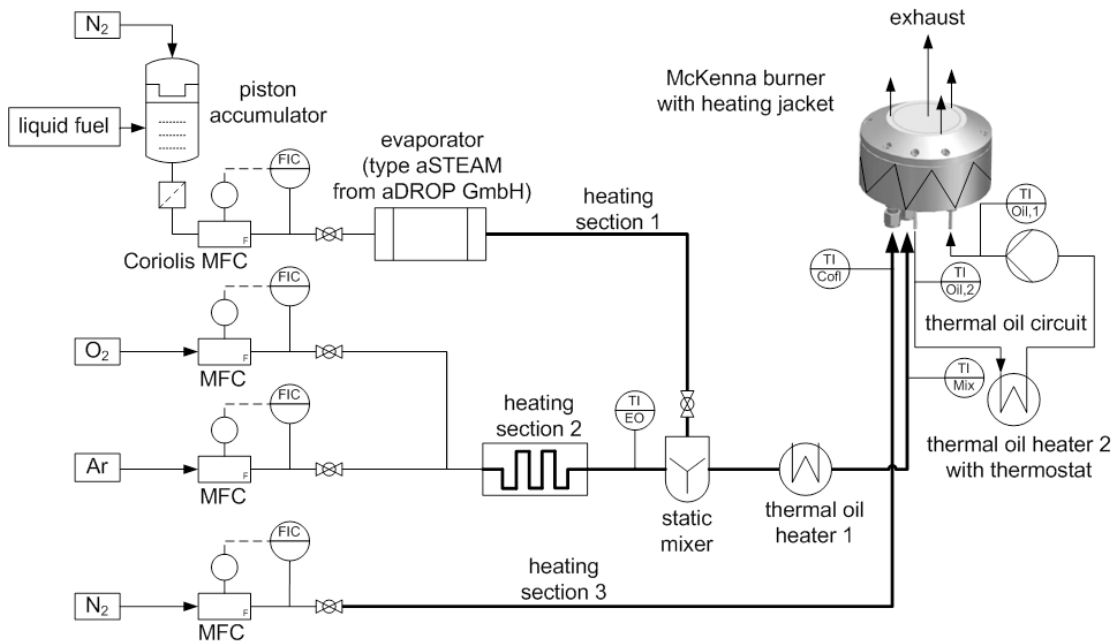
Fig. 1. Schematic of experimental setup.

The oxidizer mixture contained oxygen (purity 99.999%) and argon (purity 99.999%) as diluent. The oxygen content in the oxidizer mixture was set to 29 vol.-% due to flame stability requirements. The nitrogen used as shroud gas and as dilution gas for the sampling of the soot-loaden flame gas has a purity of 99.8%.

Table 1. Flame conditions.

Fuel	ϕ	Unburned mole fraction of mixture x_i				
		C_8H_{18}	C_2H_5OH	C_4H_9OH	O_2	Ar
reference flame						
E0/B0	2.3	0.0507	-	-	0.2753	0.6740
iso-octane/ethanol flames						
E20	2.3	0.0422	0.0303	-	0.2690	0.6585
E40	2.3	0.0331	0.0632	-	0.2621	0.6417
E65	2.3	0.0204	0.1086	-	0.2526	0.6184
E85	2.3	0.0092	0.1490	-	0.2441	0.5977
E100	2.3	-	0.1819	-	0.2373	0.5808
iso-octane/n-butanol flames						
B20	2.3	0.0414	-	0.0182	0.2727	0.6677
B40	2.3	0.0318	-	0.0373	0.2700	0.6610
B100	2.3	-	-	0.1000	0.2610	0.6390

All gases were supplied via Bronkhorst thermal mass flow controllers and the liquid fuels iso-octane (purity 99.9%), ethanol (purity 99.9%) and n-butanol (purity 99.5%) via Bronkhorst Coriolis mass flow controllers which cause uncertainties on the resulting equivalence ratio of maximum $\Delta\phi = \pm0.03$. The flow of the liquid fuel was set by the Coriolis mass flow controller and was evaporated in an adapted direct evaporator type aSTEAM from aDROP GmbH afterwards. In order to create a homogenous mixture of the vaporized fuel and the already preheated (373 K) gaseous mixture of oxygen and argon a preheated mixing chamber, which prevents the condensation of evaporated fuel during mixing, was used. The temperature of the fuel/oxidizer mixture at the inlet of the burner was fixed at 353 K. Furthermore, all transport lines downstream the mixing chamber, the burner itself and the shroud nitrogen were preheated up to minimum 358 K as well to avoid condensation of the evaporated fuel on cold surfaces.

The realized soot particle sampling system is shown in Figure 2 and was similar to the one of Zhao et al. [14]. A ceramic sample probe tube (made of $Al_2O_3 > 99.5\%$, inner diameter 9 mm, outer diameter 10 mm) was placed horizontally above the burner. The sample orifice with a diameter of 0.3 mm was drilled in the middle of the probe tube and positioned along the centerline of the flame, facing downward towards the incoming flame gas. To draw the soot containing gas sample through the orifice, a small vacuum was realized in the sampling tube. The particle-loaden gas stream was diluted immediately by a particle-free nitrogen flow at room temperature (30 l_n/min) resulting in a quenching to a temperature of around 315 K. The dilution ratio (DR) of the resulting turbulent flow (mean Reynolds number Re = 5000) in the sampling probe was DR > 10^4. This dimension was reported to be necessary in order to prevent particle losses caused by coagulation and diffusive wall deposition in the sampling line [14,15,16]. After the probe tube, the sample flow was split into two streams, a small portion of 1.5 l_n/min entering the SMPS and a large portion exhausted by a pump. In order to regulate the pressure in the sample probe and thus to adjust the applied dilution ratio, a secondary clean air stream with adjustable flow rate was introduced. The resulting dilution ratio in this study was chosen to be DR $\sim2\cdot10^4$, leading to an unavoidable uncertainty of $< \pm24\%$. Further information concerning the estimation of the dilution ratio from the pressure difference across the orifice can be found in [14]. The applied dilution ratio was proved to be right measuring and comparing the CO concentrations in the undiluted and the diluted flame gas of an ethylene flame within the framework of preliminary investigations. The mean residence time of the highly diluted sample from the probe orifice to the SMPS inlet was approximately 420 ms.

The soot particle size distributions were measured with a commercial SMPS (TSI Model 3936) which consists of a Kr-85 bipolar charger, a nano differential mobility analyzer (nano-DMA TSI Model 3085) and a condensation particle counter (CPC TSI Model 3775). This equipment enables the measurement of mobility particle diameters in the range of 2 nm to 66 nm. However, the smallest reliably detectable particle size was 4 nm (counting efficiency higher than 50%). Using the parameterized correlation between the mobility diameter and the particle diameter of a carbonaceous particle from [17,18], the measured mobility particle diameters were transformed into physical particle diameters to compare them directly with the numerical results. The resulting size distribution measurements were corrected for particle losses [19]. At least three samples of each flame were measured and a mean size distribution was calculated in order to correct statistical discordant values.
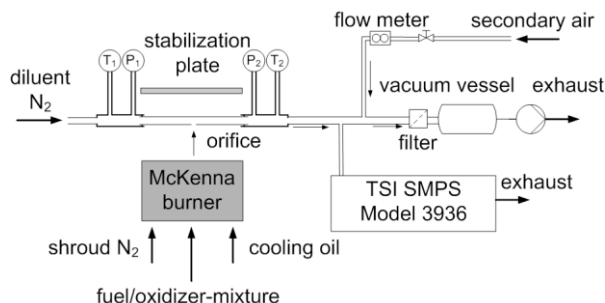

Fig. 2. Schematic of gas sampling and conditioning system for soot measurements.

The McKenna burner itself was mounted on a vertical traversing system in order to adjust the distance between sampling orifice and burner surface. The different heights above the burner correspond to different residence times and thus the progress of the chemical reactions can be followed by performing measurements at different heights above the burner. A horizontal traversing system was used to allow access to the orifice in the sampling probe for regularly cleaning of the same. The accuracy of both the vertical and the horizontal positioning was better than ±0.02 mm.

To provide the axial temperature profiles of the investigated flames, flame temperature measurements were conducted using a type S sheath thermocouple with a diameter of 0.5 mm, coated with Mg-PSZ to avoid catalytic effects on the thermocouple tip during temperature measurement in the flame. The measured axial temperature profiles were corrected for radiation losses subsequently [20] and the error in the measured temperature was maximum ±80 K.

3. Results and discussion

In Figure 3 the PSDFs of soot sampled from six iso-octane/ethanol blends (left graphs) and four iso-octane/n-butanol blends (right graphs), including the pure fuels, at three representative heights above the burner, HAB = 6 mm, 8 mm and 12 mm, are presented.
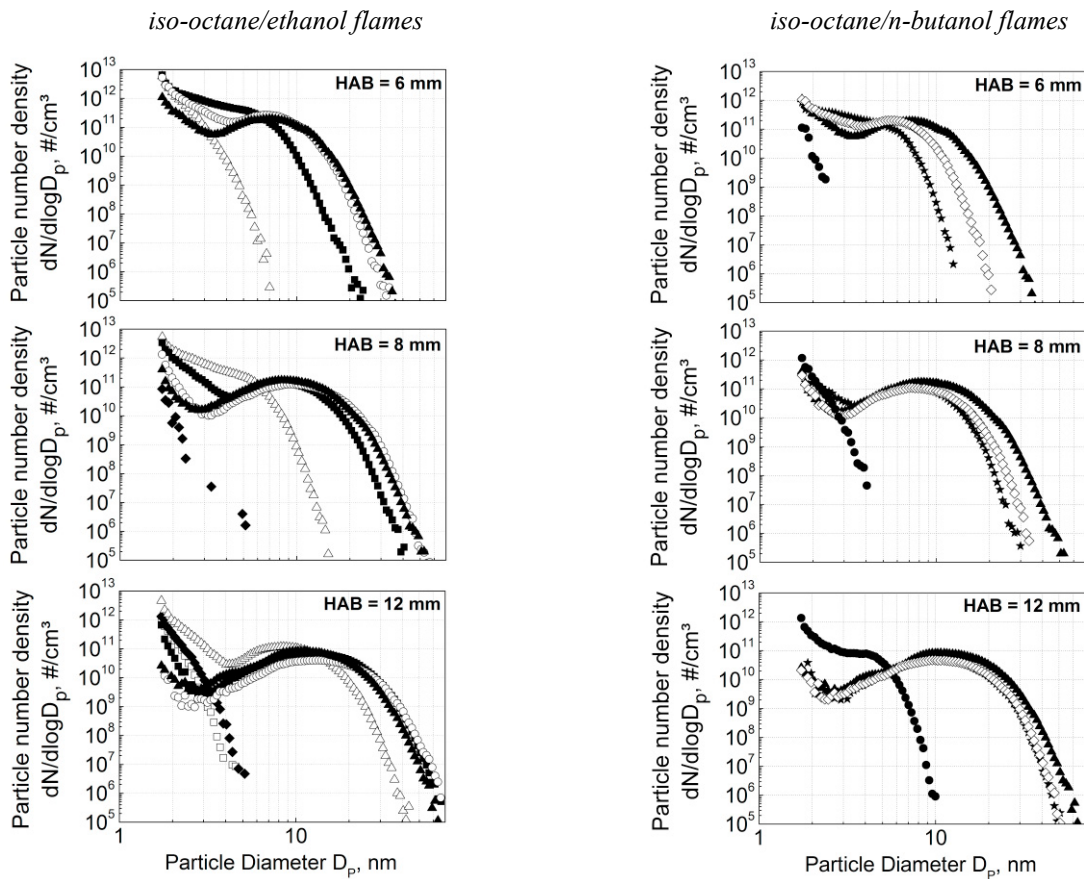

Fig. 3. Variation of PSDFs in left: E0 (▲), E20 (○), E40 (■), E65 (△), E85 (♦) and E100 (□) flames and right: B0 (▲), B20 (◊), B40 (□), B100 (●) flames ($\phi = 2.3$) at three HABs.

The PSDFs in the iso-octane flame are bimodal for all HABs and are close to log-normal distributions, e. g. for HAB = 12 mm with a median diameter of 12 nm and a maximum diameter of 65 nm. As can be seen in the left graphs of Figure 3 a shift of the PSDFs to smaller diameters occurs with increasing ethanol content in the fuel and the bimodal distributions for E0, E20 and E40 become unimodal for E65 at HAB = 6 mm. At HAB = 12 mm the PSDFs of E0, E20 and E40 are similar and just a high amount of ethanol in the fuel (> E65) reduces significantly the soot formation. The PSDFs sampled from the pure ethanol flame indicate clearly that it is slightly sooting. The first soot was detected at HAB = 10 mm and it can be observed that soot inception is still dominant at HAB = 12 mm.

The right graphs in Figure 3 show the same trends for the influence of n-butanol addition to the reference iso-octane flame. For HAB = 6 mm and HAB = 8 mm it can be observed that soot formation in the B20 and B40 flame is reduced indicated by a shift of the PSDFs to smaller diameters. Similar to the results of the iso-octane/ethanol flames, the PSDFs of B0, B20 and B40 at HAB = 12 mm show no significant differences. The PSFD sampled from the pure n-butanol flame at HAB = 6 mm represents the characteristic shape of a particle nucleation mode with a maximum particle diameter of 2.4 nm. Further in the flame (HAB = 12 mm) a shoulder starts to grow out and the distribution becomes bimodal. The nucleation mode remains indicating sustained particle nucleation.

The addition of ethanol or n-butanol leads to the disappearance of large soot particles and therefore of the soot particle growth mode in the PSDF, but only to a slight decrease of the amount of very small particles. The measured PSDFs of the soot sampled from all studied flames show clearly that the amount of small nanoparticles with diameters < 5 nm is high and is not much influenced by alkanol addition. These particles do not contribute significantly to the total soot mass emitted but are mainly responsible for the total particle number density.

In Figure 4 the measured and radiation-corrected flame temperature profiles and the profiles of the soot volume fractions and total number densities in the pure iso-octane, ethanol and n-butanol flames are plotted as function of HAB, exemplarily.
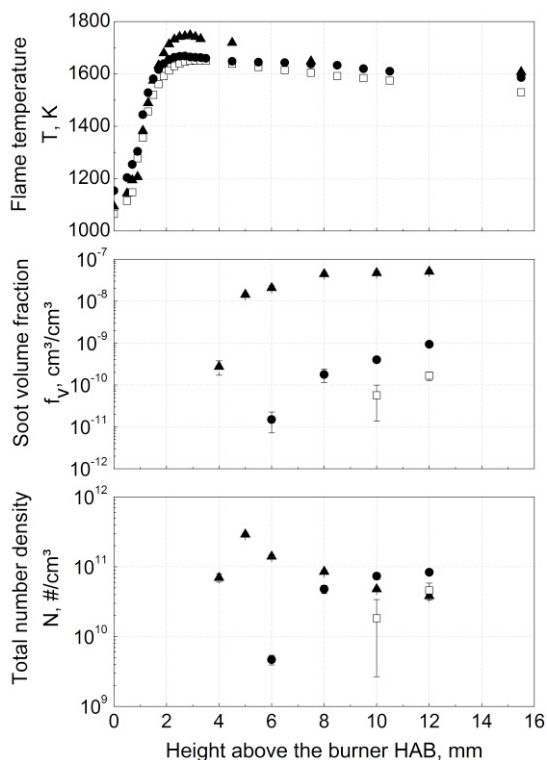

Fig. 4. Radiation-corrected axial flame temperature profile (top), soot volume fraction (middle) and total number density (bottom) in E0/B0 (▲), E100 (□) and B100 (●) flames (ϕ = 2.3).

Soot volume fractions and number densities were calculated from the PSDFs. The first stable and reproducible PSDF in the iso-octane flame was measured at HAB = 4 mm, in the n-butanol flame at HAB = 6 mm and in the ethanol flame at HAB = 10 mm. As can be expected from the PSDFs, the soot volume fraction in the iso-octane flame increases exponentially over the entire distance measured and reached a value of $5.1 \cdot 10^{-8}$ cm³/cm³ at HAB = 12 mm. The soot volume fraction in the n-butanol flame at the same HAB is reduced to 2% of this value ($9.4 \cdot 10^{-10}$ cm³/cm³) and in the ethanol flame to 0.3% ($1.7 \cdot 10^{-10}$ cm³/cm³), respectively. The total number density profile in the is-octane flame shows the often observed "first rise, then fall" behavior. The initial rise caused by particle nucleation is followed by the maximum of around $2.9 \cdot 10^{11}$ #/cm³ at HAB = 5 mm and levels off later in the flame due to balanced coagulation and particle nucleation in the upper flame region. The total number densities in all three flames are in the same order of magnitude at HAB = 12 mm with the highest value of $8.4 \cdot 10^{10}$ #/cm³ in the n-butanol flame.

Salamanca et al. [11,21] observed the same effect during their experimental investigations with premixed ethylene/ethanol flames and stated that the reason for the selectivity of ethanol in reducing particles on the basis of their size is the slow-down of the coagulation process leading to soot. The bonded oxygen in the ethanol enhances the fuel oxidation and therefore PAH and precursor nanoparticle formation are reduced. Therefore the following process of soot formation by coagulation and surface addition on the particle nuclei is less effective.

Figure 5 summarizes the soot volume fractions of all studied flames at four different HABs comparing the soot formation in the iso-octane/ethanol and iso-octane/n-butanol flames with each other. A general reduction of the total volume fraction of generated soot can be observed when an alkanol is added, with an increasing reduction as a function of the amount of ethanol and n-butanol, respectively. The trend for the iso-octane/ethanol flames shows that up to E40 the reduction is prominent just for low HABs and at HAB = 10 mm the differences in the soot volume fractions of E0, E20 and E40 are within the measurement accuracy. However, for the fuels E65, E85 and E100 the reduction of the soot volume fraction compared to pure iso-octane E0 is prominent for all HABs. The reason for this effect is that in highly sooting flames like the studied iso-octane flame surface reactions control the final amount of soot and therefore the role of ethanol addition on the reduction of soot is less effective. In slightly sooting flames like the E85 flame the effect is more evident due to the fact that the inception process controls the final amount of soot [21].
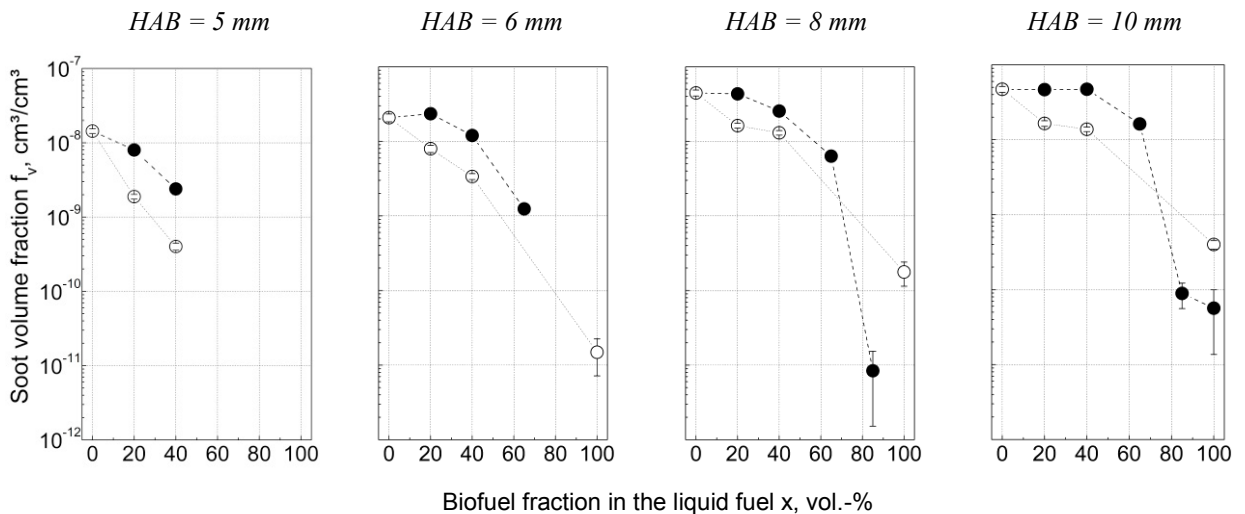

Fig. 5. Variation of soot volume fractions in all iso-octane/ethanol (filled symbols) and iso-octane/n-butanol (open symbols) flames at four HABs.

The soot volume fractions in the flames with n-butanol addition (B20, B40, B100) indicate the same behavior except that the soot reduction is obvious already for low amounts of added n-butanol for all HABs. Comparing the influence of ethanol and n-butanol on the soot formation in iso-octane flames shows that the soot volume fractions in the iso-octane/ethanol flames are higher for low amounts of added ethanol (E20, E40 and E65). For higher amounts (E85) and pure ethanol (E100) it can be observed that the reduction in the soot volume fraction is higher in the flames with ethanol than with n-butanol.

4. Conclusions

Combustion soot formed in fuel-rich laminar premixed iso-octane/ethanol and iso-octane/n-butanol flames was quantitatively characterized by probe sampling followed by particle sizing using an SMPS. The experimental work focused on the detailed understanding of how the addition of the two alkanols to the reference fuel iso-octane influences the soot formation process and especially the soot particle size distribution. The results show that the addition reduces the soot formation potential in the flames. The comparison of the soot particle size distributions of iso-octane, ethanol, n-butanol and the investigated blends for the same flame conditions indicates that both the process of soot particle nucleation in the lower heights of the flame and the coagulation process in the larger heights are influenced by the positive effect of the addition of the oxygenated fuel. This results in a reduction of the total soot volume fraction and the soot particle diameter, however, not significantly in a decrease of the total particle number. Very small soot particles have a stronger effect on health compared to larger soot particles and therefore the addition of high amounts of biofuels like ethanol or n-butanol to a fossil fuel might lead to new difficulties especially concerning the soot formation in the combustion process.

References

[1] International Energy Agency. Technology roadmap. Biofuels for Transport; 2011.
[2] Lee J, Patel R, Schönborn A, Ladommatos N, Bae C. Energy and Fuels 23; 2009; 4363–4369.
[3] Szybist JP, Youngquist AD, Barone TL, Storey JM, Moore WR, Foster M, Confer K. Energy and Fuels 25; 2011; 4977–4985.
[4] Storey JM, Barone T, Thomas J, Huff S. SAE Technical Paper; 2012 [2012-01-0437].
[5] Storch M, Hinrichsen F, Wensing M, Will S, Zigan L. Applied Energy 156; 2015; 783-792.
[6] Chen L, Stone R. Energy and Fuels 25; 2011; 1254–1259.
[7] Daniel R, Xu H, Wang C, Richardson D, Shuai S. Applied Energy 105; 2013; 252–261.
[8] Karavalakis G, Short D, Vu D, Villela M, Asa-Awuku A, Durbin TD. Fuel 128; 2014; 410–21.
[9] Lee K, Seong H, Sakai S, Hageman M, Rothamer D. SAE Technical Paper; 2013 [2013-24-0185].
[10] Wu J., Song KH, Litzinger T, Lee SY, Santoro R, Linevsky M, Colket M, Liscinsky D. Combustion and Flame 144; 2006; 675-687.
[11] Salamanca M, Sirignano M, Commodo M, Minutolo P, D'Anna A. Experimental Thermal and Fluid Science 43; 2012; 71-75.
[12] Camacho J, Lieb S, Wang H. Proceedings of the Combustion Institute 34; 2013; 1853-1860.
[13] The McKenna Flat Flame Burner. Holthuis & Associates. P.O. Box 1531, Sebastopol, CA 95473.
[14] Zhao B, Yang Z, Wang J, Johnston MV, Wang H. Aerosol Sci. Technol. 37; 2003; 611-620.
[15] Öktem B, Tolocka MP, Zhao B, Wang H, Johnston MV. Combustion and Flame 142; 2005; 364 – 373.
[16] Maricq M, Harris SJ, Szente JJ. Combustion and Flame 132; 2003; 328 – 342.
[17] Singh J, Patterson RI, Kraft M, Wang H. Combustion and Flame 145; 2006; 117 – 127.
[18] Zhao B, Yang Z, Li Z, Johnston MV, Wang H. Proceedings of the Combustion Institute 30; 2005; 1441 – 1448.
[19] Hinds W. Aerosol Technology. Wiley, New York; 1999.
[20] Shaddix C. Correcting thermocouple measurements for radiation loss: a critical review. Proceedings of the 33rd National Heat Transfer Conference; 1999.
[21] Salamanca M, Sirignano M, D'Anna A. Energy Fuels 26; 2012; 6144-6152.